Heterogeneous myocyte enhancer factor-2 (Mef2) activation in myocytes predicts focal scarring in hypertrophic cardiomyopathy

Tetsuo Konno[a], Dan Chen[a,1], Libin Wang[a], Hiroko Wakimoto[b], Polakit Teekakirikul[a], Matthew Nayor[a], Masataka Kawana[a], Seda Eminaga[a], Joshua M. Gorham[a], Kumar Pandya[c], Oliver Smithies[c], Francisco J. Naya[d], Eric N. Olson[e], J. G. Seidman[a,2,3], and Christine E. Seidman[a,f,g,2,3]

[a]Department of Genetics and [f]Howard Hughes Medical Institute, Harvard Medical School, Boston, MA 02115; [b]Department of Cardiology, Children's Hospital Boston, Harvard Medical School, Boston, MA 02115; [c]Department of Pathology and Laboratory Medicine, University of North Carolina, Chapel Hill, NC 27599; [d]Program in Cell and Molecular Biology, Department of Biology, Boston University, Boston, MA 02215; [e]Department of Molecular Biology, University of Texas Southwestern Medical Center, Dallas, TX 75390; and [g]Cardiovascular Division, Brigham and Women's Hospital, Boston, MA 02115

Unknown molecular responses to sarcomere protein gene mutations account for pathologic remodeling in hypertrophic cardiomyopathy (HCM), producing myocyte growth and increased cardiac fibrosis. To determine if hypertrophic signals activated myocyte enhancer factor-2 (Mef2), we studied mice carrying the HCM mutation, myosin heavy-chain Arg403Gln, (MHC$^{403/+}$) and an Mef2-dependent β-galactosidase reporter transgene. In young, prehypertrophic MHC$^{403/+}$ mice the reporter was not activated. In hypertrophic hearts, activation of the Mef2-dependent reporter was remarkably heterogeneous and was observed consistently in myocytes that bordered fibrotic foci with necrotic cells, MHC$^{403/+}$ myocytes with Mef2-dependent reporter activation reexpressed the fetal myosin isoform (βMHC), a molecular marker of hypertrophy, although MHC$^{403/+}$ myocytes with or without βMHC expression were comparably enlarged over WT myocytes. To consider Mef2 roles in severe HCM, we studied homozygous MHC$^{403/403}$ mice, which have accelerated remodeling, widespread myocyte necrosis, and neonatal lethality. Levels of phosphorylated class II histone deacetylases that activate Mef2 were substantially increased in MHC$^{403/403}$ hearts, but Mef2-dependent reporter activation was patchy. Sequential analyses showed myocytes increased Mef2-dependent reporter activity before death. Our data dissociate myocyte hypertrophy, a consistent response in HCM, from heterogeneous Mef2 activation and reexpression of a fetal gene program. The temporal and spatial relationship of Mef2-dependent gene activation with myocyte necrosis and fibrosis in MHC$^{403/+}$ and MHC$^{403/403}$ hearts defines Mef2 activation as a molecular signature of stressed HCM myocytes that are poised to die.

fibrosis | hypertrophy | sarcomere protein gene mutation

Hypertrophic cardiomyopathy (HCM)-causing mutations in the myosin heavy-chain gene stimulate myocyte hypertrophy, disarray, and fibrosis, the pathologic features of HCM (1). Because germline mutations cause HCM, expression of mutant sarcomere proteins is predicted to occur in all ventricular myocytes. Nonetheless, the histopathologic manifestations in human HCM are strikingly heterogeneous, and regions of marked hypertrophic remodeling abut regions with preserved myocardial architecture. Pathologic remodeling in HCM increases myocardial fibrosis, which reflects expansion of the interstitial matrix and accumulation of foci of replacement fibrosis (myocardial scarring) that arise after premature myocyte death (2, 3). Patchy myocyte death and myocardial scarring in HCM hearts have been attributed to regional ischemia (4, 5), increased ventricular wall forces (5), and impaired metabolism (6). Recent data demonstrate a correlation between the load of focal fibrosis and arrhythmias (7), an important substrate for sudden death in HCM. Moreover, myocardial scarring may contribute to the development of heart failure, which occurs in 10–15% of HCM patients (8).

Definition of the molecules and pathways in HCM that promote death or enable survival of mutant myocytes has been hampered by a lack of molecular markers that distinguish premorbid from viable mutant myocytes. To address this conundrum, we studied a mouse model of HCM that carries a sarcomere gene mutation, develops pathologic remodeling including myocyte hypertrophy and increased myocardial fibrosis (9), and exhibits diastolic dysfunction (10). As in human patients, cardiac fibrosis in HCM mice is patchy and varies in extent and distribution (11).

The myocyte enhancer factor-2 (Mef2) family of transcription factors is activated in several myocardial pathologies that are characterized by hypertrophy and fibrosis (12–15). Mef2 activation leads to reexpression of some fetal genes (12, 13, 16) that may provide compensatory adaptations (e.g., metabolic changes) that promote survival in stressed myocytes (13).

To consider whether Mef2 participates in myocyte responses to a sarcomere gene mutation, we used a genetic strategy. Mice that express a human HCM mutation, myosin heavy-chain Arg403Gln, (MHC$^{403/+}$) and a reporter of global Mef2 activity, Mef2-LacZ (β-galactosidase) (17), were characterized. Although this reporter can be activated by both Mef2 and Tead transcription factors (18), transcriptional analyses of MHC$^{403/+}$ hearts indicated a primal role for Mef2 isoforms in reporter activation. To accentuate stress from mutant sarcomeres, we also studied homozygous mutant (MHC$^{403/403}$) mice that undergo profound and relentless pathologic remodeling until death, which consistently occurs by day 10 (3). Our findings revealed marked heterogeneity in Mef2-dependent reporter activation in mutant myocytes. Activation of the Mef2-dependent reporter was unrelated to myocyte hypertrophy but was closely associated with fetal gene reexpression and focal pathological remodeling, including myocyte necrosis and myocardial scarring. Mef2-dependent gene activation provides a molecular marker that identifies premorbid myocytes and the presumptive sites of myocardial scarring in HCM.

MEDICAL SCIENCES

Results

Focal Activation of Mef2-Dependent Reporter Adjacent to Fibrotic Areas in Hypertrophic MHC[403/+] Hearts.

Cardiac hypertrophy and pathologic remodeling evolves slowly in MHC[403/+] mice, becoming overt by age 30 wk (9). Comprehensive analyses of RNAs showed that ventricular levels of Mef2a, -c and -d isoforms (Table S1) are unchanged in young, prehypertrophic MHC[403/+] and WT mice (19). With the emergence of hypertrophic remodeling, ventricular levels of Mef2a and Mef2d and phosphorylated class II histone deacetylases (HDACs), which participate in Mef2 activation (20–22), increased significantly. In comparison with Mef2a, -c, and -d isoforms, ventricular TEA domain (Tead; isoforms 1–4) transcripts were expressed at lower levels, were comparable in prehypertrophic MHC[403/+] and WT mice, and were unaltered by hypertrophic remodeling. From these data, we deduced that activation of the Mef2-dependent promoter LacZ transgene (designated Mef2-LacZ) (17) that occurred in the context of temporal remodeling in HCM reflected Mef2 activation.

Mef2-LacZ and MHC[403/+] mice were bred to generate compound MHC[403/+]/Mef2-LacZ mice. To assess Mef2-dependent reporter activity, we initially compared β-galactosidase activity in 3-wk-old MHC[403/+]/Mef2-LacZ mice and WT mice carrying the Mef2-LacZ reporter gene (designated WT/Mef2-LacZ). Left ventricular wall thickness and cardiac histology were normal in juvenile MHC[403/+]/Mef2-LacZ mice (Table S2). Light microscopy of X-gal–stained whole hearts and sections revealed comparable low levels of Mef2-dependent reporter activity (visualized as blue staining) in MHC[403/+]/Mef2-LacZ and WT/Mef2-LacZ hearts (Fig. 1A). Quantitative assessment of total Mef2-dependent reporter activity in ventricular lysates showed no difference between WT and MHC[403/+] genotypes (4.5 ± 0.37 U/mg and 6.8 ± 1.2 U/mg, respectively, P = not significant) (Fig. 1B).

At age 30 wk, MHC[403/+]/Mef2-LacZ mice had increased ventricular wall thickness (Table S2) and typical HCM cardiac histopathological abnormalities, while age-matched WT-Mef2-LacZ hearts were normal. X-gal–stained whole hearts and myocardial sections of MHC[403/+]/Mef2-LacZ mice showed more Mef2-dependent reporter activity with strikingly focal staining than seen in whole hearts and myocardial sections of WT/Mef2-LacZ mice (Fig. 1A). Quantitative assessments revealed 1.5-fold greater Mef2-dependent reporter activity (Fig. 1B) in hypertrophic MHC[403/+]/Mef2-LacZ ventricles (12.6 ± 1.6 U/mg) than in WT/Mef2-LacZ ventricles (8.1 ± 0.15 U/mg; P = 0.03).

We compared the pattern of Mef2-dependent reporter activation and histological abnormalities in left ventricular sections of hypertrophic 30-wk-old MHC[403/+]/Mef2-LacZ mice and age-matched WT/Mef2-LacZ mice, using X-gal (dark blue) and Gomori trichrome (light blue) stains, which detect collagen that accompanies fibrosis. Hypertrophic MHC[403/+]/Mef2-LacZ hearts exhibited clusters of myocytes with activated Mef2-dependent reporter, which were juxtaposed to every focal region of myocardial scarring [Fig. 2 A (see c, e, and f) and B]. In contrast, only isolated myocytes with Mef2-dependent reporter activity were detected in WT/Mef2-LacZ hearts (see a and b in Fig. 2A) and in nonscarred regions of hypertrophic MHC[403/+]/Mef2-LacZ hearts (see d in Fig. 2A). The distribution of clustered myocytes with Mef2-dependent reporter activation varied among mice and showed no consistent pattern within left ventricular segments (e.g., septum, free wall, or apex).

Because focal fibrosis or microscopic myocardial scars are assumed to emerge after myocyte death, we asked if Mef2-dependent reporter activation was associated with myocyte demise. Ventricular sections from hypertrophic MHC[403/+]/Mef2-LacZ hearts were reacted with von Kossa stain, which detects secondary dystrophic calcification, a surrogate marker of necrotic cell death. Over 50 fibrotic areas from hearts of MHC[403/+]/Mef2-LacZ mice that were more than 30 wk old (n = four mice and >20 sections per
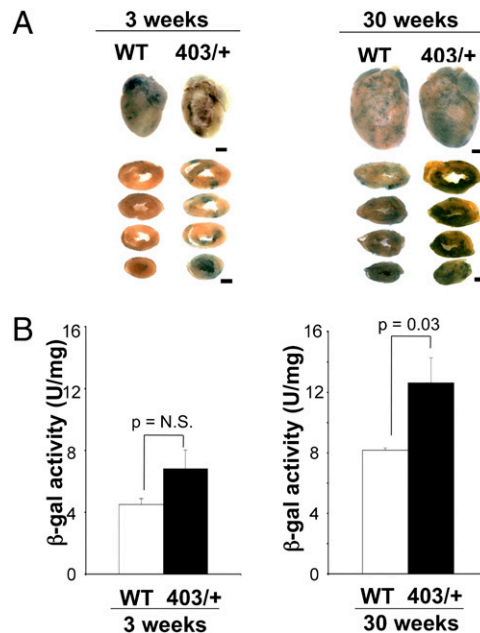
Fig. 1. Cardiac Mef2 activation in 30-wk-old MHC[403/+]/Mef2-LacZ mice (403/+) and WT/Mef2-LacZ mice (WT). (A) Whole heart and sections from mice (age 3 and 30 wk) stained with X-gal to assess β-galactosidase activity (stained blue). Left ventricles of 30-wk-old MHC[403/+] mice had increased, patchy Mef2 activation compared with WT hearts. (Scale bars: 1 mm.) (B) β-Galactosidase activity in 3- and 30-wk-old MHC[403/+] mouse ventricles compared with age-matched WT hearts (n = 3–4 per group).

mouse) were studied. Myocytes with Mef2-dependent reporter activity clustered around von Kossa staining (see b in Fig. 2B) in MHC[403/+]/Mef2-LacZ hearts, and revealed a close association of Mef2-dependent reporter activity, focal necrosis with dystrophic calcification, and scar (see a and b in Fig. 2B; X-gal plus Gomori trichrome staining and X-gal plus von Kossa staining).

Previous studies demonstrated that focal fibrosis occurs in aging WT mouse hearts (23). Consistent with these data, we observed
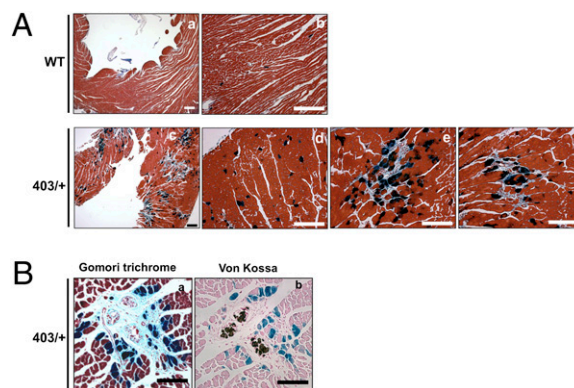
Fig. 2. Focal Mef2-reporter activation in myocytes adjacent to regions of myocardial scarring in hypertrophic MHC[403/+] mice. (A) Sections from 30-wk-old WT/Mef2-LacZ hearts (WT) and MHC[403/+]/Mef2-LacZ hearts (403/+) stained with X-gal and Gomori trichrome show increased Mef2-dependent reporter activity (dark blue) adjacent to regions of fibrosis (light blue) in 403/+ hearts (c, e, and f) compared with WT hearts (a and b). Nonclustered Mef2-dependent reporter activity was detected in nonfibrotic regions in 403/+ hearts (d). (Scale bars: 100 μm.) (B) Colocalization of Mef2-dependent reporter activity with fibrosis (a) and necrosis (b) in 30-wk-old MHC[403/+]/Mef2-LacZ hearts (403/+). Adjacent sections were stained with Xgal staining followed by Gomori trichrome staining (a) and von Kossa staining (b). (Scale bars: 100 μm.)

modest activation of the Mef2-dependent reporter near fibrotic regions in 60-wk-old WT/Mef2-LacZ hearts (Fig. S1).

βMHC Expression in Hypertrophic MHC[403/+]/Mef2-LacZ/βMHC-YFP Hearts. The cardiac fetal myosin isoform, βMHC, a molecular marker of hypertrophy, can be induced with Mef2 activation (24). To determine if the βMHC gene was reexpressed selectively in mutant myocytes with Mef2-dependent reporter activation, we crossed MHC[403/+]/Mef2-LacZ mice with transgenic mice that express YFP under control of the βMHC promoter (βMHC-YFP mice) (23). Myocytes expressing YFP were found in regions of myocardial scarring (detected by wheat germ agglutinin; WGA) (Fig. 3A). To investigate whether MHC[403/+] myocytes expressing YFP were more hypertrophic than YFP-negative myocytes, cell sizes were assessed. The average cross-sectional area of myocytes from 30-wk-old MHC[403/+]/Mef2-LacZ/βMHC-YFP mice was greater than that of age-matched WT myocytes (Fig. 3B), but there was no significant difference in the area of YFP-positive MHC[403/+] myocytes and YFP-negative MHC[403/+] myocytes (Fig. 3C). In addition, distribution and dispersion of cross-sectional areas was similar in YFP-positive MHC[403/+] myocytes and YFP-negative MHC[403/+] myocytes (Fig. S2).

To determine if activated Mef2 and βMHC were coexpressed in the same myocyte, we assessed colocalization of YFP and LacZ in 30-wk-old MHC[403/+]/Mef2-LacZ/βMHC-YFP hearts. More than 90% of myocytes that activated the Mef2-dependent reporter also expressed βMHC-promoted YFP (Fig. 3 D and E), whereas 62% of YFP-positive cells coexpressed the Mef2-dependent reporter (Fig. 3 D and E).

We concluded that Mef2 activation and βMHC expression occur in a subset of MHC[403/+] myocytes, independent of hypertrophic size, and that clusters of myocytes with Mef2 activation are juxtaposed to foci of fibrosis in MHC[403/+] hearts.
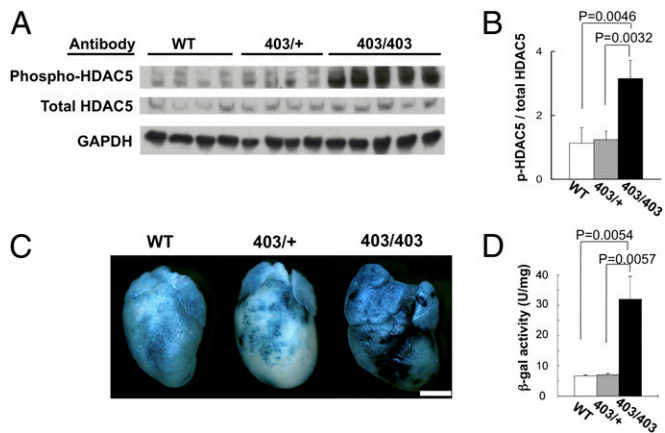
Phosphorylation of Class II HDAC in MHC[403/+] and MHC[403/403] Hearts. Calcium/calmodulin-dependent protein kinase II and protein kinase D participate in Mef2 activation by phosphorylating the repressor of Mef2, class II HDACs (20–22). We assessed phosphorylation of class II HDACs in response to the MHC[403] mutation by analyzing HDAC5 Serine 498 phosphorylation in hearts from 6-d-old WT, MHC[403/+], and MHC[403/403] mice. At this age WT and MHC[403/+] mice have normal cardiac histology, but homozygous MHC[403/403] mice have rampant cardiomyopathy with extensive pathologic remodeling and heart failure that causes death by postnatal day 10 (3). Western blots (Fig. 4 A and B) showed comparable levels of phosphorylated HDAC5 in young WT and MHC[403/+] hearts but significantly elevated levels in homozygous MHC[403/403] hearts (WT vs. MHC[403/403], $P = 0.0046$; MHC[403/+] vs. MHC[403/403], $P = 0.0032$).

HDAC5 Serine-498 phosphorylation also was assessed in hearts from 3-wk-old and 30-wk-old WT and MHC[403/+] mice (Fig. S3). Phosphorylated HDAC5 levels were indistinguishable in 3-wk-old WT and MHC[403/+] hearts, but at 30 wk, when hypertrophic remodeling is evident in MHC[403/+] hearts, phosphorylation levels of HDAC5 was significantly increased in MHC[403/+] hearts compared with WT hearts ($P = 0.03$).

Mef2-Dependent Reporter Activation and Myocyte Necrosis in Homozygous MHC[403/403] Hearts. Given the markedly increased phosphorylated HDAC5 in MHC[403/403] mice, we assessed Mef2-dependent reporter activation in MHC[403/403]/Mef2-LacZ mice. Six-day-old homozygous mutant mice had more X-gal staining (Fig. 4C) and 4.8-fold increased β-galactosidase activity (Fig. 4D)
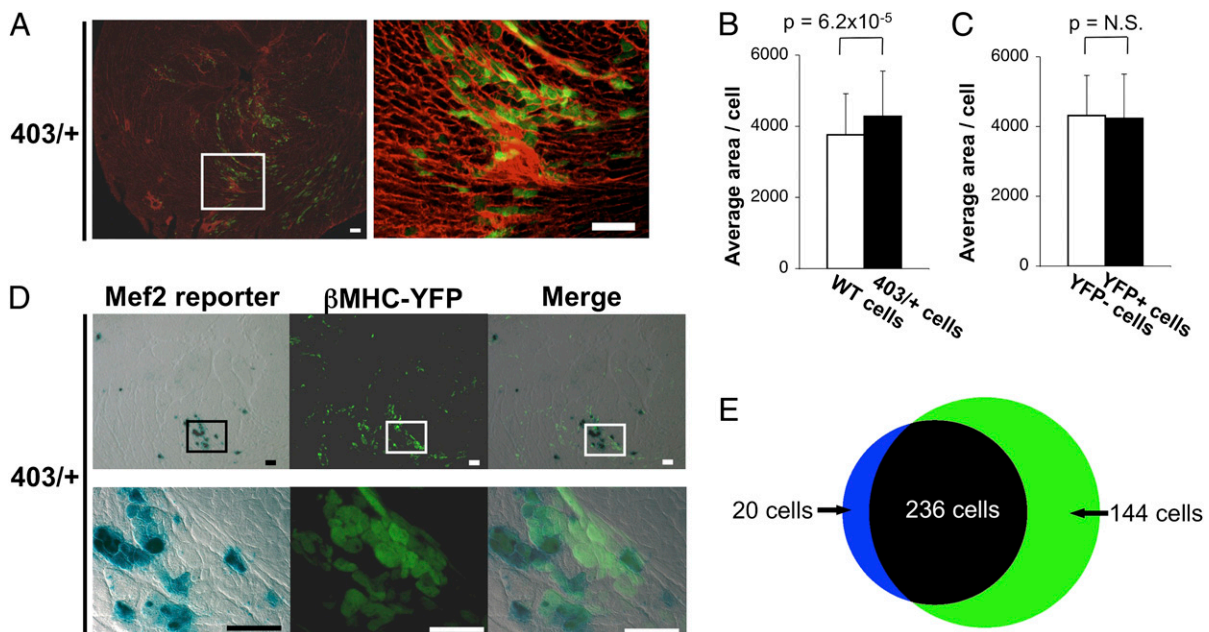
Fig. 3. Colocalization of Mef2-dependent reporter activity and fetal gene reexpression in MHC[403/+] myocytes adjacent to a myocardial scar. (A) βMHC reexpression (identified by YFP) occurred in regions of myocardial scars (identified by WGA) in 30-wk-old MHC[403/+]/Mef2-LacZ /βMHC-YFP hearts (403/+). *Right* shows magnified view of boxed area in *Left*. (Scale bars: 100 μm.) (B) Cross-sectional areas of myocytes from 30-wk-old WT/Mef2-LacZ/βMHC-YFP hearts (WT cells; open bar) and MHC[403/+]/Mef2-LacZ / MHC-YFP hearts (403/+ cells; black bars) irrespective of their fluorescence. (C) Cross-sectional areas of the 403/+ cells grouped according to their YFP fluorescence (YFP- and YFP+, respectively). Over 200 cells per group were analyzed. (Fig. S2 shows distribution of cross-sectional areas of YFP⁻ cells and YFP⁺ cells.) (D) Colocalization of Mef2-dependent reporter activity and βMHC-YFP reexpression in 30-wk-old MHC[403/+]/Mef2-LacZ/βMHC-YFP hearts. The majority of cells are positive for both Mef2-dependent reporter activity and βMHC-YFP; few cells express only one. Lower row shows boxed areas in upper rows at higher magnification. (Scale bars: 100 μm.) (E) Quantitative assessment of Mef2-dependent reporter activity and βMHC-YFP expression in 256 myocytes; 92% (236 myocytes) coexpressed the Mef2-dependent reporter and βMHC-YFP. Blue, myocytes positive only for Mef2-dependent reporter activity; green, myocytes positive only for βMHC-YPF; black, myocytes positive for both.
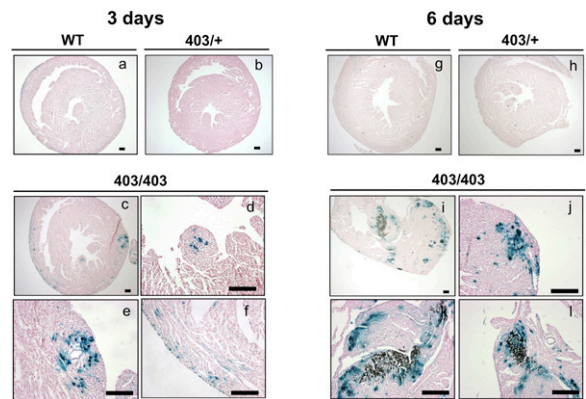
Fig. 4. Increased phosphorylation of HDAC5 and Mef2-dependent reporter activity in MHC$^{403/403}$ hearts. (*A*) Western blots of heart lysates from 6-d-old WT, MHC$^{403/+}$ (403/+), and MHC$^{403/403}$ (403/403) mice, reacted with antibodies specific for HDAC5 serine-498, total HDAC5, and GAPDH. (*B*) Phospho-HDAC5 was normalized to total HDAC5 (*n* = four to five mice per group). (*C*) X-gal–stained (blue) hearts from 6-d-old WT/Mef2-LacZ (WT), MHC$^{403/+}$/Mef2-LacZ (403/+), and MHC$^{403/403}$/Mef2-LacZ (403/403) mice. MHC$^{403/403}$/Mef2-LacZ hearts had heterogeneous and greater activation of the MEF2-dependent reporter than WT and MHC$^{403/+}$ hearts. (Scale bar: 1 mm.) (*D*) β-Galactosidase (β-gal) activity (*Materials and Methods*) measured in hearts from 6-d-old WT/Mef2-LacZ (WT), MHC$^{403/+}$/Mef2-LacZ (403/+), and MHC$^{403/403}$/Mef2-LacZ (403/403) mice. β-Galactosidase activity was significantly increased in MHC$^{403/403}$ hearts compared with WT and MHC$^{403/+}$ hearts (*n* = three per group).

Fig. 5. Mef2-reporter activity is associated with necrotic tissue in homozygous MHC$^{403/403}$ hearts. Sections from 3-d-old hearts from WT/Mef2-LacZ (*A*), MHC$^{403/+}$/Mef2-LacZ (*B*), and MHC$^{403/403}$/Mef2-LacZ mice (*C–F*) and 6-d-old hearts from WT/Mef2-LacZ (*G*), MHC$^{403/+}$/Mef2-LacZ (*H*), and MHC$^{403/403}$/Mef2-LacZ mice (*J–L*) stained with X-gal (blue) and von Kossa stain (brown). A representative 3-d-old MHC$^{403/403}$/Mef2-LacZ mouse heart (*C–F*) demonstrated that activation of the Mef2-dependent reporter occurred before onset of necrosis. Focal Mef2-dependent reporter activity without necrosis also was detected in 6-d-old MHC$^{403/403}$ hearts (*J*). Note that necrosis occurred in the myocardium where the Mef2-dependent reporter had been activated in 6-d-old MHC$^{403/403}$ hearts (*K* and *L*). Other images from 6-d-old MHC$^{403/403}$ hearts are shown in Fig. S4. (Scale bars: 100 μm.)

than either WT/Mef2-LacZ or MHC$^{403/+}$/Mef2-LacZ hearts (WT vs. MHC$^{403/403}$, *P* = 0.0054; MHC$^{403/+}$ vs. MHC$^{403/403}$, *P* = 0.0057). Even when the dosage of mutant myosins was doubled, β-galactosidase activity was not found in all MHC$^{403/403}$ myocytes.

The rapidly progressive cardiomyopathy of MHC$^{403/403}$ mice afforded the opportunity to assess the temporal relationship of Mef2-dependent reporter activation and myocyte necrosis. Histopathologic sections of 3-d-old WT/Mef2-LacZ, MHC$^{403/+}$/Mef2-LacZ, and MHC$^{403/403}$/Mef2-LacZ hearts showed no dystrophic calcification, a marker of necrosis (Fig. 5 *A–F*). Mef2-dependent reporter activity was virtually absent from WT/Mef2-LacZ and MHC$^{403/+}$/Mef2-LacZ hearts (Fig. 5 *A* and *B*), but focal activation of the Mef2-dependent reporter occurred in MHC$^{403/403}$/Mef2-LacZ hearts (Fig. 5 *C–F*). At postnatal day 6, WT/Mef2-LacZ and MHC$^{403/+}$/Mef2-LacZ hearts lacked detectable Mef2-dependent reporter activity or necrosis (Fig. 5 *G* and *H*). However, 6-d-old MHC$^{403/403}$/Mef2-LacZ hearts had abundant, patchy Mef2-dependent reporter activity in myocytes surrounding necrotic foci (Fig. 5 *I–L* and Fig. S4) and in myocytes without nearby necrosis (Fig. 5*I*). Based on the consistent activation of Mef2-dependent reporter in advance of necrotic death of MHC$^{403/403}$ myocytes and the colocalization of activated Mef2-dependent reporter, fibrosis, and myocyte necrosis in MHC$^{403/+}$ hearts, we concluded that activation of the Mef2-dependent reporter delineated profoundly stressed mutant ventricular myocytes at risk for premature death.

Atrial Activation of the Mef2-Dependent Reporter. The Mef2-dependent reporter also was activated in atria from 6-d-old MHC$^{403/403}$ and hypertrophic MHC$^{403/+}$ mice. Atrial activation of the reporter was absent in 6-d-old WT/Mef2-LacZ and MHC$^{403/+}$/Mef2-LacZ hearts (Fig. S5 *A* and *B*) but was robust in left and right atria of 6-d-old MHC$^{403/403}$/Mef2-LacZ mice (Fig. S5 *C–F*). Mef2-dependent reporter activation occurred occasionally in atrial myocytes from 30-wk-old WT/Mef2-LacZ mice (Fig. S5 *G* and *H*), but was substantially greater in atrial myocytes from hypertrophic MHC$^{403/+}$/Mef2-LacZ hearts (Fig. S5 *I–L*). Unlike ventricular

specimens, there was neither dystrophic calcification nor focal fibrosis nearby atrial myocytes with Mef2-dependent reporter activation.

Discussion

We demonstrate markedly heterogeneous activation of an Mef2-dependent reporter in myocytes with the HCM mutation MHC^{403}. Activation of Mef2 correlated with reexpression of the fetal myosin isoform βMHC but was independent of the hypertrophic size of mutant ventricular myocytes. In MHC$^{403/403}$ hearts, temporal activation of the Mef2-dependent reporter preceded ventricular myocyte death, but in MHC$^{403/+}$ hearts Mef2-dependent reporter activation in ventricular myocytes was closely associated with foci of necrosis and replacement fibrosis. Together these data define Mef2 activation in HCM as a molecular marker of stressed myocytes that are at risk for premature death. As such, Mef2-dependent gene activation in the HCM heart often occurs in regions destined to develop focal myocardial scarring, a histopathologic hallmark of this cardiomyopathy.

Heterogeneous Mef2 Activation in HCM. Unexpectedly we found that a germline HCM mutation in genetically inbred mice elicited different transcriptional response in myocytes throughout the myocardium. Mef2-dependent gene activation in HCM hearts was not global but occurred in random patches, a finding that suggests three conclusions. First, because hypertrophic MHC$^{403/+}$ myocytes had comparable size regardless of Mef2-dependent reporter activation or βMHC expression, myocyte growth signals in HCM appear to be independent of an Mef2 transcriptional program. Second, that Mef2 activation occurred in variable ventricular locations of identical mice suggests that regional parameters, such as intrinsic coronary vasodilator reserve (25) or hemodynamic forces (5), are unlikely to drive myocyte death and the subsequent emergence of microscopic myocardial scarring in HCM hearts. Third, the substantial concordance between activation of Mef2-dependent reporter and expression of the fetal βMHC isoform provided the potential for a direct benefit to HCM myocytes: dilution of the amount of mutant protein within the sarcomere and an associated reduction in adverse cellular consequences. Nevertheless, Mef2-dependent gene activation in

myocytes was closely associated with ventricular myocyte death, indicating inadequate compensation to the stress imposed by a sarcomere gene mutation (Fig. 6). We assume that the pathways involved in pressure-overload activation of the fetal βMHC isoform (23) also participate in activation of Mef2.

Mef2 Pathway to Myocardial Necrosis and Scarring in HCM. Premature death of myocytes and replacement by focal myocardial scar is widely recognized in human HCM and in model organisms (2, 3), but molecules that promote death or survival in mutant myocytes have not been identified previously. Our data define Mef2 activation as a marker that distinguishes HCM myocytes. Although the intrinsic level of Mef2 activity in myocytes may be more pervasive than is measured by the reporter construct used here, the Mef2-dependent reporter provided a critical tool for differentiating mutant myocytes. Ventricular myocytes with Mef2-dependent reporter activation were consistently juxtaposed to foci of necrotic myocyte cells (Fig. 2 and Fig. 5 *I–L*), implicating Mef2 activation as a molecular barometer of stress in HCM myocytes. A similar role has been postulated in other cardiac pathologies (12). That Mef2-dependent reporter was activated before widespread myocyte death in homozygous MHC$^{403/403}$ hearts (Fig. 5 *I–L*) further supports this model. Moreover, the correlation between levels of Mef2-dependent reporter activation and mutation dosage suggests that stress is graded within myocytes, because activation was substantially less in hearts carrying a single mutant allele of myosin than in hearts with two mutant alleles. By extrapolation to human HCM, we predict that Mef2-dependent gene activation would be particularly high in myocytes with compound sarcomere gene mutations that produce severe histopathology and an associated deleterious clinical course (1, 26). Defining cell and molecular properties of myocytes with robust Mef2 activation therefore may inform opportunities to reduce stress and promote survival in HCM.

Two major cardiac Mef2 isoforms, Mef2a and Mef2d, were increased in response to the MHC^{403} mutation (Table S1). Although either isoform, or both, would account for the activation of the Mef2-dependent reporter used in these studies, the increased activation of Mef2a or Mef2d might have different consequences on HCM hearts. The MHC^{403} mutation produces profound biophysical changes within the sarcomere (27, 28), alters myocyte handling of calcium (29), and produces a wide range of molecular and cellular responses (19) that increase energy demands in HCM hearts (28). Increased transcription of Mef2a could provide metabolic compensation for these intrinsic stresses by regulating mitochondrial biogenesis (15), regulating the insulin-responsive glucose transporter type 4 (30), and activating genes that enable myocytes to use glucose instead of fatty acids for energy production (12, 13, 16).

Myocytes with sarcomere mutations also engender responses in their local milieu, including expansion of the interstitial matrix. Mef2d has been implicated in transcriptional activation of genes encoding extracellular matrix proteins, including connective tissue growth factor and procollagen (types I and III) (13). Remodeling of the interstitium may lead to impaired myocyte relaxation and increased hypoxia due to decreased capillary density and increased oxygen diffusion distances (25, 28). Alternatively, remodeling of the extracellular matrix may be beneficial in HCM, as has been demonstrated in wound healing (31).

Whether Mef2 provides adaptive or maladaptive responses in HCM likely depends on isoform involvement and duration of activation. The robust activation of the Mef2-dependent reporter in atria that occurred without myocyte necrosis (Fig. S5 *I–L*) implies adaptive responses. However, because other models have demonstrated that continued Mef2-dependent gene activation is deleterious (13), we speculate that prolonged Mef2 activation contributes to pathologic atrial remodeling that occurs in both HCM mice (3, 9) and human patients (32). In contrast to activation in atrial myocytes, ventricular Mef2-dependent gene activation
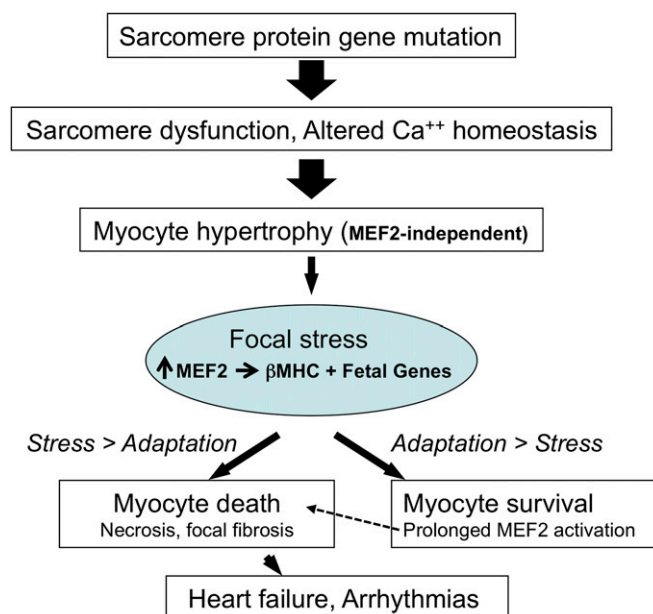
Fig. 6. A pathway from mutation to focal fibrosis in HCM. Mutant sarcomere proteins trigger hypertrophy in most myocytes (broad arrow). Stressed myocytes activate Mef2 and express downstream target genes including βMHC. When Mef2-dependent gene activation inadequately compensates for stresses, myocytes die (necrosis), and focal myocardial scars emerge. Prolonged activation of Mef2-dependent genes fosters survival (34) but may become maladaptive (13), contributing to pathological remodeling. Accumulation of focal fibrosis (33, 35) may promote adverse outcomes in HCM, including heart failure and arrhythmias.

occurred in myocytes that were closely associated with focal necrosis and myocardial scarring (Figs. 2B and 5 *I–L*). Even adaptive Mef2-dependent gene activation may be inadequate to compensate for the stress of sarcomere gene mutations in ventricular myocytes, which, because of higher ventricular force, probably are subject to greater stress than atrial myocytes. We suggest that balance between the duration of Mef2 activation and myocyte stress is critical in myocyte survival or death in HCM hearts (Fig. 6).

An important and unresolved question is why Mef2-dependent gene activation was strikingly inhomogeneous. Somatic differences in allelic expression of the mutant gene or in posttranscriptional regulation of mutant mRNAs and protein might alter the level of dominant mutation in myocytes. Different levels of molecules that respond to sarcomere gene mutations [i.e., calcium-handling proteins, proteins involved in energetics, and growth factors (19)] also might compensate for or exacerbate the consequences of HCM mutations in myocytes. Alternatively, paracrine signaling by growth factors (i.e., TGF-β) derived from interstitial cardiac fibroblasts may influence Mef2 activation in myocytes (33). Regardless of the mechanism leading to Mef2 activation, we suggest that patchy Mef2 activation involves class II, specifically HDAC5, phosphorylation (Fig. 4), because increased HDAC5 phosphorylation was observed in both hypertrophic MHC$^{403/+}$ and MHC$^{403/403}$ hearts. With Mef2-dependent gene activation as a molecular tool to discriminate between healthy and stressed mutant myocytes, definition of cellular responses that result in pathologic remodeling from sarcomere gene mutations will be feasible.

In conclusion, Mef2-dependent gene activation is not the primary molecular trigger for hypertrophy in HCM but rather is a signature of focal stress. Mef2-dependent gene activation defines myocytes in which pathways leading to myocyte death and focal myocardial scarring, a major histopathologic feature of HCM, have been activated. Studies to determine if inhibition or

MEDICAL SCIENCES

activation of Mef2a and Mef2d can attenuate pathological remodeling may provide new clues regarding the susceptibility to arrhythmias and development of heart failure in HCM.

Materials and Methods

Mouse Models. Heterozygous MHC[403/+] mice and homozygous MHC[403/403] mice have been described previously (3, 9, 29). Mef2-LacZ mice carrying a LacZ transgene controlled by three tandem copies of the Mef2 binding site (17) and βMHC-YFP mice carrying YFP knocked in to the βMHC locus have been described previously (23). MHC[403/+]/Mef2-LacZ, MHC[403/403]/Mef2-LacZ, and MHC[403/+]/Mef2-LacZ/βMHC-YFP mice were derived by mating mutant strains. All mice were maintained according to protocols approved by the Institutional Animal Care and Use Committee of Harvard Medical School.

Assessment of β-Galactosidase Activity and Histochemical Analyses. Total Mef2 activity in ventricular tissue extracts from WT/Mef2-LacZ, MHC[403/+]/Mef2-LacZ, and MHC[403/403]/Mef2-LacZ mice were determined by a qualitative histochemical assay. Hearts were fixed in 2% paraformaldehyde/0.2% glutaraldehyde in PBS on ice for 60 min and then were immersed overnight at 37 °C in β-galactosidase staining solution [5 mM ferrocyanide, 5 mM ferricyanide, 2 mM MgCl2, 1 mg/mL X-gal (5-bromo-4-chloro-3-indolyl-b-ᴅ-galactopyranoside) in dimethylformamide]. Heart tissues subsequently were processed for histopathological analyses. Paraffin-embedded sections were stained with either Gomori trichrome to detect collagen or von Kossa stain to detect secondary dystrophic calcification associated with necrotic tissue. Quantitative measurements of β-galactosidase activity (14) were made with the β-galactosidase assay kit (Stratagene).

The βMHC-YFP fusion protein was detected by fluorescence. Heart tissues from βMHC-YFP mice were embedded in the optimal cryo temperature compound on dry ice. Sections (10 μm) were cut at −20 °C and mounted on Superfrost Plus microscope slides. βMHC-YFP protein expression and myocardial scarring was assessed for colocalization in sections stained with fluorescent WGA, labeled with Alexa Fluor 599 (Invitrogen), and images were acquired with a Leica microscope. βMHC-YFP and Mef2-LacZ expression was visualized in the same section by LacZ staining (light microscopy) and by detecting YFP signal with fluorescence microscopy.

Cross-Sectional Areas of Myocytes. Individual YFP-βMHC–positive and –negative myocytes were visualized in WGA-stained MHC[403/+]/MEF2-LacZ/βMHC-YFP heart sections, and their cross-sectional area was measured by ImageJ software as described previously (23). Myocytes from age- and gender-matched WT mice were studied in parallel.

Immunoblot Analyses. Western blots were performed as described previously (3, 14), using primary antibodies rabbit anti-phospho-HDAC5 (1:500; Abcam) and rabbit anti-total HDAC5 (1:100; Cell Signaling Technology).

Statistical Analysis. Data were expressed as means ± SE. Differences between groups were determined by unpaired Student's t test or one-factor ANOVA. A P value <0.05 was considered statistically significant.

1. Ingles J, et al. (2005) Compound and double mutations in patients with hypertrophic cardiomyopathy: Implications for genetic testing and counselling. *J Med Genet* 42: e59.
2. Maron BJ, Spirito P (1998) Implications of left ventricular remodeling in hypertrophic cardiomyopathy. *Am J Cardiol* 81:1339–1344.
3. Fatkin D, et al. (1999) Neonatal cardiomyopathy in mice homozygous for the Arg403Gln mutation in the alpha cardiac myosin heavy chain gene. *J Clin Invest* 103: 147–153.
4. Tanaka M, et al. (1987) Quantitative analysis of narrowings of intramyocardial small arteries in normal hearts, hypertensive hearts, and hearts with hypertrophic cardiomyopathy. *Circulation* 75:1130–1139.
5. Knaapen P, et al. (2008) Determinants of coronary microvascular dysfunction in symptomatic hypertrophic cardiomyopathy. *Am J Physiol Heart Circ Physiol* 294: H986–H993.
6. Tuunanen H, et al. (2007) Myocardial perfusion, oxidative metabolism, and free fatty acid uptake in patients with hypertrophic cardiomyopathy attributable to the Asp175Asn mutation in the alpha-tropomyosin gene: A positron emission tomography study. *J Nucl Cardiol* 14:354–365.
7. Adabag AS, et al. (2008) Occurrence and frequency of arrhythmias in hypertrophic cardiomyopathy in relation to delayed enhancement on cardiovascular magnetic resonance. *J Am Coll Cardiol* 51:1369–1374.
8. Spirito P, Maron BJ, Bonow RO, Epstein SE (1987) Occurrence and significance of progressive left ventricular wall thinning and relative cavity dilatation in hypertrophic cardiomyopathy. *Am J Cardiol* 60:123–129.
9. Geisterfer-Lowrance AA, et al. (1996) A mouse model of familial hypertrophic cardiomyopathy. *Science* 272:731–734.
10. Georgakopoulos D, et al. (1999) The pathogenesis of familial hypertrophic cardiomyopathy: Early and evolving effects from an alpha-cardiac myosin heavy chain missense mutation. *Nat Med* 5:327–330.
11. Wolf CM, et al. (2005) Somatic events modify hypertrophic cardiomyopathy pathology and link hypertrophy to arrhythmia. *Proc Natl Acad Sci USA* 102: 18123–18128.
12. Zhang CL, et al. (2002) Class II histone deacetylases act as signal-responsive repressors of cardiac hypertrophy. *Cell* 110:479–488.
13. Kim Y, et al. (2008) The MEF2D transcription factor mediates stress-dependent cardiac remodeling in mice. *J Clin Invest* 118:124–132.
14. Zhang T, et al. (2007) CaMKIIdelta isoforms differentially affect calcium handling but similarly regulate HDAC/MEF2 transcriptional responses. *J Biol Chem* 282: 35078–35087.
15. Naya FJ, et al. (2002) Mitochondrial deficiency and cardiac sudden death in mice lacking the MEF2A transcription factor. *Nat Med* 8:1303–1309.
16. Potthoff MJ, Olson EN (2007) MEF2: A central regulator of diverse developmental programs. *Development* 134:4131–4140.
17. Naya FJ, Wu C, Richardson JA, Overbeek P, Olson EN (1999) Transcriptional activity of MEF2 during mouse embryogenesis monitored with a MEF2-dependent transgene. *Development* 126:2045–2052.
18. Yoshida T (2008) MCAT elements and the TEF-1 family of transcription factors in muscle development and disease. *Arterioscler Thromb Vasc Biol* 28:8–17.
19. Kim JB, et al. (2007) Polony multiplex analysis of gene expression (PMAGE) in mouse hypertrophic cardiomyopathy. *Science* 316:1481–1484.
20. Backs J, Song K, Bezprozvannaya S, Chang S, Olson EN (2006) CaM kinase II selectively signals to histone deacetylase 4 during cardiomyocyte hypertrophy. *J Clin Invest* 116: 1853–1864.
21. Backs J, et al. (2009) The delta isoform of CaM kinase II is required for pathological cardiac hypertrophy and remodeling after pressure overload. *Proc Natl Acad Sci USA* 106:2342–2347.
22. Fielitz J, et al. (2008) Requirement of protein kinase D1 for pathological cardiac remodeling. *Proc Natl Acad Sci USA* 105:3059–3063.
23. Pandya K, Kim HS, Smithies O (2006) Fibrosis, not cell size, delineates beta-myosin heavy chain reexpression during cardiac hypertrophy and normal aging in vivo. *Proc Natl Acad Sci USA* 103:16864–16869.
24. van Oort RJ, et al. (2006) MEF2 activates a genetic program promoting chamber dilation and contractile dysfunction in calcineurin-induced heart failure. *Circulation* 114:298–308.
25. Petersen SE, et al. (2007) Evidence for microvascular dysfunction in hypertrophic cardiomyopathy: New insights from multiparametric magnetic resonance imaging. *Circulation* 115:2418–2425.
26. Tsoutsman T, Bagnall RD, Semsarian C (2008) Impact of multiple gene mutations in determining the severity of cardiomyopathy and heart failure. *Clin Exp Pharmacol Physiol* 35:1349–1357.
27. Tyska MJ, et al. (2000) Single-molecule mechanics of R403Q cardiac myosin isolated from the mouse model of familial hypertrophic cardiomyopathy. *Circ Res* 86: 737–744.
28. Spindler M, et al. (1998) Diastolic dysfunction and altered energetics in the alphaMHC403/+ mouse model of familial hypertrophic cardiomyopathy. *J Clin Invest* 101:1775–1783.
29. Fatkin D, et al. (2000) An abnormal Ca(2+) response in mutant sarcomere protein-mediated familial hypertrophic cardiomyopathy. *J Clin Invest* 106:1351–1359.
30. Sparling DP, Griesel BA, Weems J, Olson AL (2008) GLUT4 enhancer factor (GEF) interacts with MEF2A and HDAC5 to regulate the GLUT4 promoter in adipocytes. *J Biol Chem* 283:7429–7437.
31. Murphy G, Nagase H (2008) Reappraising metalloproteinases in rheumatoid arthritis and osteoarthritis: Destruction or repair? *Nat Clin Pract Rheumatol* 4:128–135.
32. Sanada H, et al. (1993) Increased left atrial chamber stiffness in hypertrophic cardiomyopathy. *Br Heart J* 69:31–35.
33. Manabe I, Shindo T, Nagai R (2002) Gene expression in fibroblasts and fibrosis: Involvement in cardiac hypertrophy. *Circ Res* 91:1103–1113.
34. Rajabi M, Kassiotis C, Razeghi P, Taegtmeyer H (2007) Return to the fetal gene program protects the stressed heart: A strong hypothesis. *Heart Fail Rev* 12: 331–343.
35. Sabbah HN, Sharov VG, Lesch M, Goldstein S (1995) Progression of heart failure: A role for interstitial fibrosis. *Mol Cell Biochem* 147:29–34.